

# Parameter extraction of solar cell models using mutative-scale parallel chaos optimization algorithm<sup>☆</sup>

Xiaofang Yuan<sup>\*</sup>, Yongzhong Xiang, Yuqing He

*College of Electrical and Information Engineering, Hunan University, Changsha 410082, China*

Received 22 February 2014; received in revised form 10 July 2014; accepted 11 July 2014

Available online 31 July 2014

Communicated by: Associate Editor Arturo Morales-Acevedo

## Abstract

To simulate solar cell systems or to optimize photovoltaic (PV) system performance, accurate parameter values of solar cell systems are extremely crucial. In this article, the parameter extraction of solar cell models is posed as an optimization process with an objective function minimizing the difference between the measured values and estimated data. A mutative-scale parallel chaos optimization algorithm (MPCOA) using crossover operation and merging operation is proposed for this optimization problem. To verify the performance of MPCOA, it is applied to extract the parameters of different solar cell models, i.e., double diode, single diode, and PV module. Comparison results with other parameter extraction techniques are in favor of the MPCOA, which signifies its potential as another optional method.

© 2014 Elsevier Ltd. All rights reserved.

**Keywords:** Solar cell models; Photovoltaic (PV) system; Parameter extraction; Parallel chaos optimization algorithm (PCOA)

## 1. Introduction

The utilization of renewable energy has experienced steady increase over the past years due to limited supply of fossil fuels and air pollution. Solar energy is one of the most promising renewable energy sources due to readily available, easy installation, low maintenance, and almost zero pollution (Chan et al., 1986; Zhou et al., 2007; Sandrolini et al., 2010). With the increasing utilization of solar energy, researches on photovoltaic (PV) generation system have received significant attention in the past few years (Amrouche et al., 2012; Tian et al., 2012; Khan

et al., 2013; Orioli and Gangi, 2013; Cubas et al., 2014). To simulate solar cell systems or to optimize PV systems performance, accurate parameter values of these systems are extremely crucial.

In the past decades, various parameters extraction techniques, such as nonlinear fitting algorithms (Easwarakhanthan et al., 1986; Kim and Choi, 2010), analytical solution methods (Saleem and Karmalkar, 2009; Jain and Kapoor, 2004), have been developed and proposed to extract various parameters of solar cell models. According to different mathematical representations, analytical solution methods applied in this field can be classified to two main types: one type is approximate analytical methods (Saleem and Karmalkar, 2009) which are usually expressed in terms of elementary functions, the other type is exact analytical methods (Jain and Kapoor, 2004) based on the Lambert W-function which cannot be expressed in terms of elementary functions.

<sup>☆</sup> This work was supported in part by the National Natural Science Foundation of China (No. 61104088) and Young Teachers Promotion Program of Hunan University.

<sup>\*</sup> Corresponding author.

E-mail address: [yuanxiaofang126@126.com](mailto:yuanxiaofang126@126.com) (X. Yuan).

Due to the non-linearity, multi-variable and multi-modal features of solar cell models, it is difficult for these techniques to accurately extract the unknown parameters. As a result, artificial intelligence (AI) techniques, such as artificial neural network (ANN) or fuzzy logic based intelligent modeling techniques (AbdulHadi et al., 2004) and meta-heuristic algorithms based parameter extraction techniques (Hachana et al., 2013), have been developed and proposed for this problem. The recent developments on this topic as well as different parameter extraction techniques are described in the following section.

Chaos optimization algorithm (COA) (Li and Jiang, 1998; Yang et al., 2007; Yuan and Wang, 2008) is a novel global optimization technique, which employs numerical sequences generated by means of chaotic maps. Due to the distinctive properties of chaotic sequences, such as sensitive dependence on initial conditions, stochasticity and ergodicity, many existing application results have demonstrated that COA escapes from local minima more easily than algorithms such as genetic algorithm (GA), simulated annealing (SA), particle swarm optimization (PSO), differential evolution (DE) and harmony search algorithm (HSA) (Okamoto and Hirata, 2013; Yang et al., 2014). In this article, a novel mutative-scale parallel chaos optimization algorithm (MPCOA) is proposed to extract parameters of solar cell models. In this article, the parameter extraction of solar cell models is posed as an optimization process which makes the difference minimum between the real data and estimated values. In order to evaluate the ability of the MPCOA, different solar cell models, i.e., double diode, single diode and PV module, have been applied. Compared with other optimization algorithms based parameter extraction techniques, the proposed MPCOA has the superiority of global optimization ability and good performance. Comparison results with other parameter extraction techniques are in favor of the MPCOA.

The rest of this article is arranged as follows. Section 2 briefly surveys recent developments in parameters extraction of solar cell models. The optimization problem for parameters extraction of solar cell models is introduced in Section 3. Section 4 gives presentation of the proposed MPCOA technique. Simulation and experiment results have been used to verify the ability of the MPCOA in Section 5. Conclusions are presented in Section 6.

## 2. Survey on recent developments in parameter extraction of solar cell models

Accurate parameter values are extremely crucial in the simulation, evaluation, control and optimization of PV systems. Consequently, a lot of techniques have been developed and proposed for this problem. A brief review of these techniques is as follows.

Firstly, conventional nonlinear fitting algorithms, such as least-squares method (LSM) and its variations, have been put forward to solve this problem. In Easwarakhanthan et al. (1986), Newton's method based modified nonlinear

LSM was proposed to extract solar cell models parameters from measured current and voltage ( $I$ – $V$ ) data, and a reduced LSM initialization routine was used to overcome the difficulties in initializing parameters. In Kim and Choi (2010), the diode  $I$ – $V$  curve was constructed by the LSM based correlation between estimated values and measured ones. The major defect of LSM fitting is its sensitivity to outliers. Outliers usually have a great impact on the fitting performance because the effect of these extreme data points is magnified by squaring the residuals.

Second, analytical solution methods have also been widely used in this field. According to different mathematical representations, analytical solution methods in this field can be classified to two main types: one type is approximate analytical methods which are commonly expressed in terms of elementary functions, the other type is exact analytical methods based on the Lambert W-function which cannot be expressed in terms of elementary functions. Karmalkar and Haneefa (2008) proposed a simple explicit current–density–voltage ( $J$ – $V$ ) model, which simplified the prediction of  $J$ – $V$  curves. Saleem and Karmalkar (2009) proposed analytical parameters extraction method which avoided the difficult measurements of  $dJ/dV$  and  $(J_p, V_p)$ . The parameters of the single exponential  $J$ – $V$  model were extracted simultaneously from measurements of open circuit voltage  $V_{oc}$ , short circuit current density  $J_{sc}$ ,  $V|_{J=0.6J_{sc}}$ , and  $J|_{V=0.6V_{sc}}$ . Das (2012) developed an analytical explicit  $J$ – $V$  solar cell model from the physics based on implicit  $J$ – $V$  equation, which was obtained by using Taylor's series expansion based algebraic manipulations. Lun et al. (2013) used Padé approximant to represent the exponential function term of  $I$ – $V$  equation, both basic and modified Padé approximants models were considered. Lun et al. (2013) developed Taylor's series expansion based explicit analytical model, which described the entire single-diode solar cell  $I$ – $V$  characteristic using two modified five-parameter models. In a few words, the main disadvantage of these approximate analytical methods is that the availability is under certain conditions, such as continuity, differentiability and convexity (AlRashidi et al., 2011). Moreover, the implementation of these methods is not easy because they typically involve heavy computation and tedious algebraic manipulation.

Nowadays, the Lambert W-function based exact analytical methods have already demonstrated useful. In mathematics, the Lambert W-function is a set of functions, namely the branches of the inverse function with the definition as:  $x = W(x)e^{W(x)}$ , for any complex number  $x$ . Many researches have demonstrated that Lambert W-function can distinctly represent the relationship between voltage  $V$ , current  $I$  and resistance  $R$  in a diode (Jain and Kapoor, 2004; Jain and Kapoor, 2005). More importantly, solutions based on Lambert W-function are not only exact and explicit but also easily differentiable. Jain and Kapoor (2004) proposed Lambert W-function based exact analytical solutions of real solar cells parameters, which were obtained by the W-function based explicit solutions. Jain

and Kapoor (2005) studied the exact explicit solutions of various parameters of organic solar cell using Lambert W-function. Ortiz-Conde and Sanchez (2005) extracted the intrinsic and extrinsic model parameters of semiconductor junctions using an integral difference function-D, which was expressed in terms of Lambert W-function. The so called “Co-content function” based on Lambert function was proposed in Ortiz-Conde et al. (2006) to extract explicit analytical solutions of the  $I$ – $V$  characteristics. Similar analytical methods based on Lambert W-function were developed in Jain et al. (2006), Bayhan and Bayhan (2011), Ghani et al. (2013), Ghani et al. (2013) for various solar cell parameters. Combination method of the Lambert W-function and polynomial curve fitting for solar cells modeling was also utilized in Chen et al. (2011), Peng et al. (2013). The main advantage of the Lambert W-functions based exact analytical methods is the realization of analytical explicit solution. However, the accuracy of exact analytical methods is at the cost of computation speed. Moreover, the precision of extracted values by these methods is greatly influenced by measurement noise.

The recent development in intelligent modeling techniques has promoted solar cell models and PV modules that take advantage of the numeric abilities of artificial neural network (ANN) or the symbolic abilities of fuzzy logic (FL). AbdulHadi et al. (2004) developed an adaptive network-based fuzzy inference system (ANFIS) based solar cell model, which represented the characteristic of solar cell arrays under various environmental conditions even with few historical measured data. Karatepe et al. (2006) investigated an ANN based PV equivalent circuit model considering solar irradiation and temperature, the inputs of ANN were solar irradiation and temperature while the outputs of ANN included  $I_{ph}$ ,  $I_s$ ,  $R_s$ ,  $R_{sh}$  and  $n$ . For dual-junction (DJ) GaInP/GaAs solar cells both at one sun and at dark levels, Patra (2011,a) proposed ANN modeling techniques to characterize their behaviors involving tunneling effect and complex interactions between the junctions. In Fathabadi (2013), the  $I$ – $V$  and  $P$ – $V$  curves of silicon/plastic solar cells and module were determined by hybrid feed-forward ANN with Lambert W-function. Syafaruddin et al. (2012) proposed a Takagi–Sugeno type fuzzy system coupled with a discrete wavelet network to determine the maximum power points (MPP) voltage of various non-crystalline silicon solar cells. In Bonanno et al. (2012), the output characteristic of a commercial PV module was estimated by radial basis function neural networks (RBFNN), whose inputs were solar irradiation and temperature values. Compared with other explicit solutions methods, ANN and FL based intelligent modeling techniques bring several benefits, such as requiring less historical measured data, arbitrary nonlinear function approximation capability. Shortcomings in intelligent modeling techniques include dependence on model structure and learning algorithm, long training times, proneness to over-fitting.

Metaheuristics and optimization algorithms have attracted much attention in the area of parameter extraction of solar cells. Compared with other techniques, metaheuristics and optimization algorithms usually define an objective function minimizing the difference between the measured values and estimated ones, as a result, the parameter extraction of solar cells is posed as an optimization process. Jervase et al. (2001) formulated the solar cell parameter extraction problem as a search and optimization one, which was implemented using genetic algorithm (GA). Zagrouba et al. (2010) applied GA to identify the electrical parameters of solar cells/PV modules, and these parameters was used to calculate the MPP. In Ye et al. (2009) and Huang et al. (2011), particle swarm optimization (PSO) method was applied to extract various solar cells parameters. The applications of pattern search (PS) technique to obtain the parameters of solar cell/PV module were developed in AlRashidi et al. (2011) and AlHajri et al. (2012), with an objective function minimizing the summation of the individual absolute error (IAE). Modified differential evolution (DE), such as penalty-based DE (Ishaque et al., 2012) and repaired adaptive DE (Gong and Cai, 2013), were also utilized for fast and accurate extraction of solar cell parameters. Other metaheuristic, such as simulated annealing (SA) (El-Naggar et al., 2012), artificial bee swarm optimization (ABSO) (Askarzadeh and Rezazadeh, 2013), hybrid artificial bee colony (ABC) with DE (Hachana et al., 2013) were also considered in this field. However, the performance of metaheuristics and optimization algorithms relies strongly on algorithm's search capability, while the above optimization algorithms usually fall in local minima.

### 3. Problem formulation

In this section, we will introduce equivalent circuit and mathematical model that represents the electrical characteristics of the solar cell and PV module.

#### 3.1. Double diode model

The equivalent circuit of a double diode model is illustrated in Fig. 1(a). In the double diode model, the cell terminal current  $I_t$  can be formulated as follows (Tian et al., 2012):

$$I_t = I_{ph} - I_{d1} - I_{d2} - I_{sh} \quad (1)$$

where  $I_{ph}$  is the photo-generated current;  $I_{d1}$  and  $I_{d2}$  denote the first and second diode current, respectively;  $I_{sh}$  denotes the shunt resistor current.

Currents  $I_{d1}$ ,  $I_{d2}$  and  $I_{sh}$  can be specifically represented according to Shockley equation, as a result, Eq. (1) is rewritten as follows (Tian et al., 2012):

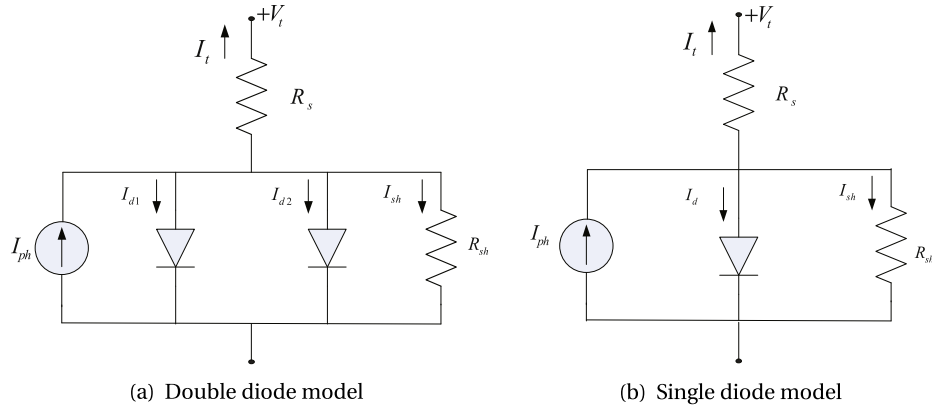


Fig. 1. Equivalent circuit of solar cell models.

$$I_t = I_{ph} - I_{sd1} \left[ \exp\left(\frac{q(V_t + R_s I_t)}{n_1 k T}\right) - 1 \right] - I_{sd2} \left[ \exp\left(\frac{q(V_t + R_s I_t)}{n_2 k T}\right) - 1 \right] - \frac{V_t + R_s I_t}{R_{sh}} \quad (2)$$

where  $V_t$  is the terminal voltage;  $I_{sd1}$  and  $I_{sd2}$  are the diffusion and saturation currents, respectively;  $R_s$  and  $R_{sh}$  are the series and shunt resistances, respectively;  $n_1$  and  $n_2$  are the diffusion and recombination diode ideality factors;  $q$  denotes the electronic charge ( $1.6 \times 10^{-19}$  C),  $k$  denotes the Boltzmann constant ( $1.38 \times 10^{-23}$  J/K), and  $T$  denotes the cell temperature (K). Given a set of measured  $V$ – $I$  data for such double diode model, seven parameters,  $R_s$ ,  $R_{sh}$ ,  $I_{ph}$ ,  $I_{sd1}$ ,  $I_{sd2}$ ,  $n_1$  and  $n_2$ , are to be extracted. For different solar cells, these parameters are varied.

### 3.2. Single diode model

The equivalent circuit of a single diode model is illustrated in Fig. 1(b). In the single diode model, with the use of non-physical diode ideality factor  $n$ , the diffusion and recombination currents are combined together. For such a single diode model, Eq. (2) is changed to the following from as (Cubas et al., 2014):

$$I_t = I_{ph} - I_{sd} \left[ \exp\left(\frac{q(V_t + R_s I_t)}{n k T}\right) - 1 \right] - \frac{V_t + R_s I_t}{R_{sh}} \quad (3)$$

Given a set of measured  $V$ – $I$  data, the parameter extraction problem for such a single diode model reduces to find five parameters:  $R_s$ ,  $R_{sh}$ ,  $I_{ph}$ ,  $I_{sd}$  and  $n$ .

### 3.3. PV module model

A typical model structure of a PV module (using single diode model) is illustrated in Fig. 2, which is effectively the interconnection of solar cells in series or/and parallel ( $N_s \times N_p$ ) configuration. The output current equation of a PV module is mathematically expressed as in the following equation (El-Naggar et al., 2012):

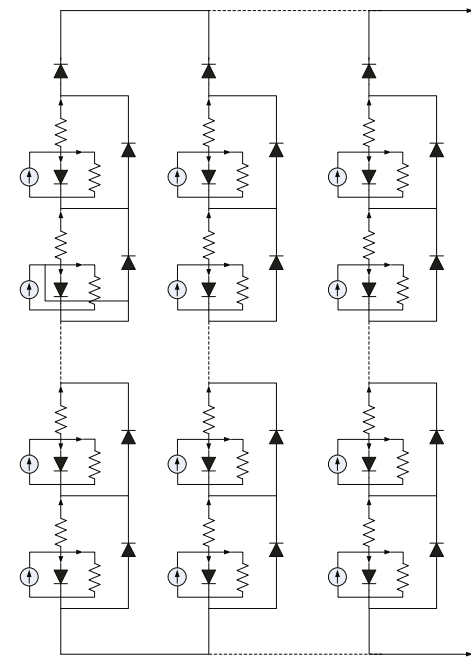


Fig. 2. Equivalent circuit model of a PV module.

$$I_t = I_{ph} N_p - I_{sd} N_p \left[ \exp\left(\frac{q\left(\frac{V_t}{N_s} + I_t \frac{R_s}{N_p}\right)}{n k T}\right) - 1 \right] - \frac{\frac{V_t N_p}{N_s} + R_s I_t}{R_{sh}} \quad (4)$$

As this PV module is comprised of series and parallel combinations using single diode model, five unknown parameters ( $R_s$ ,  $R_{sh}$ ,  $I_{ph}$ ,  $I_{sd}$  and  $n$ ) are need to be extracted as in Eq. (3).

### 3.4. Optimization problem in parameter extraction of solar cell models

In this article, the parameter extraction of solar cell models is posed as an optimization process which makes the difference minimum between the real data and estimated values. The optimization algorithms based solar



cell models parameters extraction techniques are usually implemented in the following way: a set of real  $V$ – $I$  data of solar cell or PV module is measured, an objective function minimizing the difference between the real data and estimated values is defined, then an optimization algorithm is applied to tune the parameters until the best objective function obtained. After the optimization procedure, the best solutions obtained by the optimization algorithm is just the extracted optimal parameters values.

Each solution of this problem is given by a vector  $X$ , where  $X = [R_s \ R_{sh} \ I_{ph} \ I_{sd1} \ I_{sd2} \ n_1 \ n_2]$  and  $X = [R_s \ R_{sh} \ I_{ph} \ I_{sd} \ n]$  are for the double and single diode model, respectively. For this optimization problem, an objective function needs to be defined. To define the objective function for solar cell models parameters extraction, Eqs. (2)–(4) are rewritten in their homogeneous forms as follows:

$$f(V_t, I_t, X) = I_t - I_{ph} + I_{sd1} \left[ \exp\left(\frac{q(V_t + R_s I_t)}{n_1 k T}\right) - 1 \right] + I_{sd2} \left[ \exp\left(\frac{q(V_t + R_s I_t)}{n_2 k T}\right) - 1 \right] + \frac{V_t + R_s I_t}{R_{sh}} \quad (5)$$

$$f(V_t, I_t, X) = I_t - I_{ph} + I_{sd} \left[ \exp\left(\frac{q(V_t + R_s I_t)}{n k T}\right) - 1 \right] + \frac{V_t + R_s I_t}{R_{sh}} \quad (6)$$

$$f(V_t, I_t, X) = I_t - I_{ph} N_p + I_{sd} N_p \left[ \exp\left(\frac{q\left(\frac{V_t}{N_s} + I_t \frac{R_s}{N_p}\right)}{n k T}\right) - 1 \right] + \frac{\frac{V_t N_p}{N_s} + R_s I_t}{R_{sh}} \quad (7)$$

When different solutions  $X$  are put into Eqs. (5)–(7), the calculated  $f(V_t, I_t, X)$  for each pair of  $V$ – $I$  data is mostly different. Usually, the root mean square error (RMSE) is a criterion to evaluate the difference between the real data and estimated values. Therefore, the following objective function to minimize RMSE is employed here for parameters extraction of solar cell models:

$$\text{minimize } RMSE = \sqrt{\frac{1}{M} \sum_{i=1}^M f(V_t, I_t, X)^2} \quad (8)$$

where  $M$  is the number of real  $V$ – $I$  data. The parameters extraction error will result in a nonzero objective function  $RMSE$ , which is used to guide the optimization search for better parameters vector  $X$ . If calculated  $RMSE$  is bad, the parameters vector  $X$  are tuned by the optimization algorithm and sent to Eqs. (5)–(7) again. This iterative procedure for improving the parameters vector  $X$  is usually stopped when the objective function is good enough or the optimization algorithm has reached the maximum iteration times.

#### 4. MPCOA technique

As chaos is a bounded pseudo-randomness behavior which exhibits sensitive dependence on initial conditions,

convergence of original COA is usually effected by starting points. For this reason, a kind of population-based parallel chaotic optimization algorithm (PCOA) have been developed in our former works (Yuan et al., 2012, 2014). The concept of population is applied in the PCOA, where each decision variable has been mapped by multiple chaotic sequences.

In this article, we will propose a mutative-scale parallel chaos optimization algorithm (MPCOA) with crossover and merging operation. Compared with the original PCOA, the MPCOA has two main improvements, they are, crossover operation and merging operation. Both crossover and merging operation exchange information within population and produce new potential solutions, which are different to those derived from chaotic sequences. In essence, crossover and merging operation are kinds of local exploiting search. Therefore, the MPCOA provides a good balance between exploration and exploitation.

##### 4.1. Crossover operation

Generally, motion step of chaotic sequence between two successive iteration is very big, which results in a big jump of decision variable in search space. This kind of big jump is of benefit to jump out local optimum, however it is not valid for the exact solution exploiting. In this article, the crossover operation is used for information interaction among parallel variables. The crossover operation is illustrated in Fig. 3. Two parallel variables from parallel solutions  $x_j^*$  are randomly chosen for crossover operation, and the produced new potential variables usually are different to those derived from chaotic sequences.

##### 4.2. Merging operation

In order to improve algorithm's exact solution exploiting capability, merging operation is also used in the MPCOA. The merging operation is illustrated in Fig. 4.

The merging operation between two parallel variables from parallel solutions  $x_j^*$  is denoted by:

$$x_{i1}^{(M)} = \gamma_{i1} * x_{i1}^* + (1 - \gamma_{i1}) * x_{i2}^* \quad (9)$$

where  $\gamma_{i1}$  is chaotic map, and frequently used Logistic chaotic map is defined by Li and Jiang (1998), Yang et al. (2007), Yuan and Wang (2008):

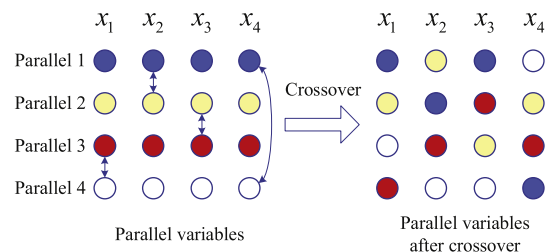


Fig. 3. Crossover operation among parallel variables.

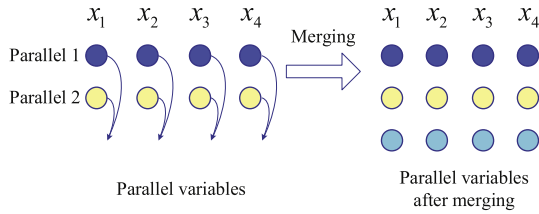


Fig. 4. Merging operation among parallel variables.

$$\gamma_{n+1} = 4\gamma_n(1 - \gamma_n), \gamma_n \in (0, 1) \quad (10)$$

Similarly to the crossover operation, two parallel variables from parallel solutions  $x_j^*$  are randomly chosen for merging operation, and the produced new potential variables usually are different to those derived from chaotic sequences.

#### 4.3. Mutative-scale search space

With the increase of iterations in MPCOA, parallel solutions  $x_j^*$  usually become gathered. So the exact solution exploiting is the main task after many iteration numbers. The mutative-scale search space is utilized in the MPCOA for exact solution exploiting. Mutative-scale search space is conducted around the so far best solution  $x_i^*$  as:

$$L'_i = x_i^* - \Phi(U_i - L_i), U'_i = x_i^* + \Phi(U_i - L_i) \quad (11)$$

where  $L_i$  and  $U_i$  are lower and upper limits, respectively;  $L'_i$  and  $U'_i$  are the corresponding contracted limits;  $\Phi$  represents a mutative-scale factor according to the iteration number  $k$  defined by:

$$\Phi = \left( \frac{k_{\max} - k}{k_{\max}} \right)^4 \quad (12)$$

In order to avoid  $L'_i$ ,  $U'_i$  beyond search space  $[L_i, U_i]$ , the updated search space is limited as follows: If  $L'_i < L_i$ , then  $L'_i = L_i$ ; if  $U'_i > U_i$ , then  $U'_i = U_i$ .

As a result, the updated search space is contracted for accurate exploiting, and the updated search space is utilized in the subsequent iteration as:

$$L_i = L'_i, U_i = U'_i \quad (13)$$

#### 4.4. MPCOA technique

Consider the optimization problem of solar cell models parameter extraction as in Eq. (8),  $X$  is the decision variables consisting of  $n$  variables  $x_i \in R^n$ . The procedure of the proposed MPCOA technique is described as follows, which is also illustrated in Fig. 5.

**Step 1:** Set MPCOA parameters: population size (parallel number)  $N$ , max iteration number  $k_{\max}$ , crossover operation rate  $P_c$ , merging operation rate  $P_m$ . Initialize parameter: parallel optimum  $P_j^* = \infty$ , global optimum  $P^* = \infty$ , random initial value of chaotic maps  $0 < \gamma_{ij}(k) < 1$ , set iteration number  $k = 1$ .

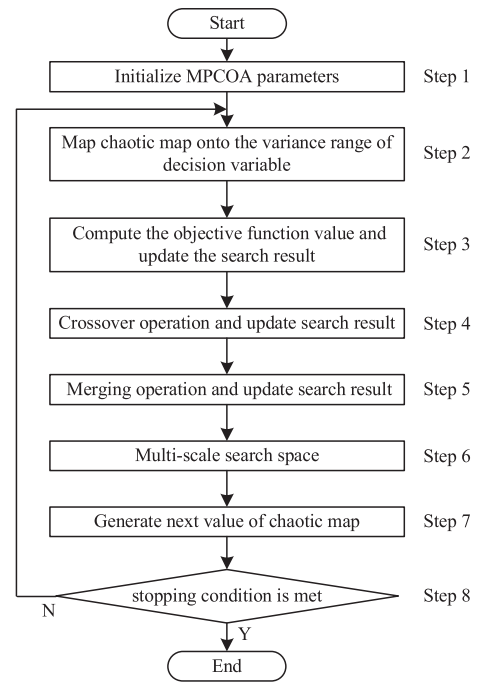


Fig. 5. Flowchart of the proposed MPCOA technique.

**Step 2:** Map chaotic map  $\gamma_{ij}(k)$  onto the variance range of decision variable  $x_{ij}(k)$  by:

$$x_{ij}(k) = L_i + \gamma_{ij}(k)(U_i - L_i). \quad (14)$$

**Step 3:** Compute the objective function value and update the search result. If  $f(X(k)) < P_j^*$ , then  $x_j^* = x_j(k)$  and parallel optimum  $P_j^* = f(X(k))$ . If  $P_j^* < P^*$ , then global optimum  $P^* = P_j^*$ , and  $X^* = x_j^*$ .

**Step 4:** Crossover operation and update the search result. The new produced parallel variables denoted by  $x_j^{(C)}$ . If  $f(X^{(C)}) < P_j^*$ , then  $x_j^* = x_j^{(C)}$  and parallel optimum  $P_j^* = f(X^{(C)})$ . If  $P_j^* < P^*$ , then global optimum  $P^* = P_j^*$ , and  $X^* = x_j^*$ .

**Step 5:** Merging operation and update the search result. The new produced parallel variables denoted by  $x_j^{(M)}$ . If  $f(X^{(M)}) < P_j^*$ , then  $x_j^* = x_j^{(M)}$  and parallel optimum  $P_j^* = f(X^{(M)})$ . If  $P_j^* < P^*$ , then global optimum  $P^* = P_j^*$ , and  $X^* = x_j^*$ .

**Step 6:** Mutative-scale search space as in Eqs. (11)–(13), then update the search space  $[L_i, U_i]$ .

**Step 7:** Generate  $k + 1$ th iteration of chaotic sequences using the chaotic map given in Eq. (10):

$$\gamma_{ij}(k + 1) = 4\gamma_{ij}(k)(1 - \gamma_{ij}(k)) \quad (15)$$

**Step 8:** If  $k \geq k_{\max}$ , stop the optimization process; otherwise  $k \leftarrow k + 1$ , go to Step 2.

In Step 4 and Step 5, both crossover operation and merging operation are used as the supplement to the MPCOA at each iteration. This means that if the new variables after crossover or merging operation have reached a better objective function value than the original ones, the new variables will replace original ones. In another situation, if the new variables bring a worse objective function value, the new variables will be given up. In order to balance the computing cost and accuracy, the crossover operation rate is  $P_c = 0.1 \sim 0.5$ , and the merging operation rate is  $P_m = 0.1 \sim 0.5$ , that is, about 10–50% of parallel variables have been executed the crossover or merging operation at each iteration.

## 5. Simulation and experiment tests

In this section, the performance of the MPCOA based parameter extraction technique is tested using measured data. Real measured  $V$ – $I$  data of solar cell and PV module are employed in this simulation. The prototype of solar cell is a 57 mm diameter commercial silicon solar cell and the  $V$ – $I$  measurements have been taken under 1 sun ( $1000 \text{ W/m}^2$ ) at  $33^\circ\text{C}$ . The prototype of PV module is 36 polycrystalline silicon cells which are connected in series and the  $V$ – $I$  measurements have been taken under 1 sun ( $1000 \text{ W/m}^2$ ) at  $45^\circ\text{C}$ . These two prototypes are the same as in AlRashidi et al. (2011) and AlHajri et al. (2012).

The adjustable parameters of the MPCOA technique in this simulation, determined by trial, are given by: population size (parallel number)  $N = 100$ , max iteration number  $k_{\max} = 2500$ , crossover operation rate  $P_c = 0.5$ , merging operation rate  $P_m = 0.5$ . During the MPCOA based optimization process, the lower and upper bounds of optimization parameters  $X$ , provided by the literature (Askarzadeh and Rezazadeh, 2013), are as follows:  $R_s(\Omega) \in [0, 0.5]$ ,  $R_{sh}(\Omega) \in [0, 100]$ ,  $I_{ph}(A) \in [0, 1]$ ,  $I_{sd}(\mu A) \in [0, 1]$ , and  $n \in [1, 2]$ .

### 5.1. Case study 1: double diode model

In this case, 26 pairs  $V$ – $I$  values as the same as in Cubas et al. (2014) are used as the measured  $V$ – $I$  data. These measurements are used for the search of optimal parameters  $X^*$  by the MPCOA. The convergence process of the MPCOA during the parameter extraction process for the double diode model is plotted in Fig. 6, indicating the global optimal value of the objective function as in Eq. (8) during the iterations.

Extracted optimal parameters values  $X^*$  and RMSE value for the double diode model of MPCOA have been reported in Table 1. Here MPCOA is compared with several other techniques, they are: artificial bee swarm optimization (ABSO) (Askarzadeh and Rezazadeh, 2013), pattern search (PS) (AlHajri et al., 2012), simulated annealing (SA) (El-Naggar et al., 2012), and harmony search algorithm (HSA) (Askarzadeh and Rezazadeh, 2013). Since it is difficult to test all parameter extraction techniques, these tech-

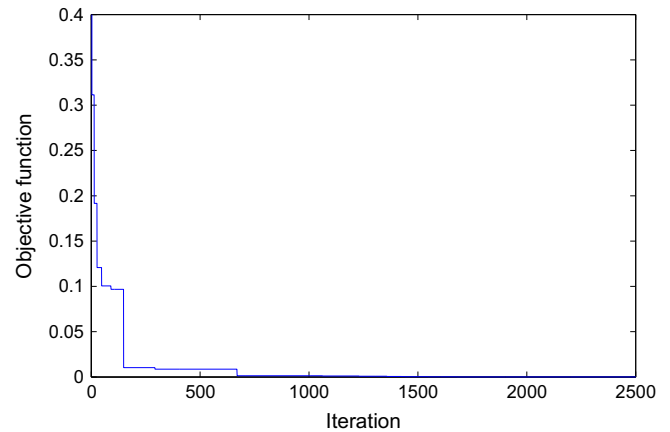


Fig. 6. Convergence process of MPCOA during the parameter extraction process.

Table 1

Comparison among different parameter extraction techniques for the double diode model.

Item	MPCOA	ABSO	PS	SA	HSA
$R_s(\Omega)$	0.03635	0.03657	0.0320	0.0345	0.03545
$R_{sh}(\Omega)$	54.2531	54.6219	81.3008	43.1034	46.8269
$I_{ph}(A)$	0.76078	0.76077	0.7602	0.7623	0.76176
$I_{sd1}(\mu A)$	0.31259	0.26713	0.9889	0.4767	0.12545
$I_{sd2}(\mu A)$	0.04528	0.38191	0.0001	0.0100	0.25470
$n_1$	1.47844	1.46512	1.6000	1.5172	1.49439
$n_2$	1.78459	1.98152	1.1920	2.0000	1.49989
RMSE	9.2163e-4	9.8344e-4	0.01518	0.01664	0.00126

niques have been chosen for comparison because they have been demonstrated with good results for parameter extraction problem.

The extracted optimal parameters values  $X^*$  and RMSE value of these techniques have been summarized in Table 1. From Table 1, we can see that the MPCOA provides the lowest RMSE value (9.2163e-4) among these techniques, followed by ABSO, HSA, PS and SA. Since MPCOA has found the minimum RMSE value, we can conclude that MPCOA outperforms ABSO, PS, SA, and HSA. As a result, the optimal values  $X^*$  found by MPCOA are closer to the real ones for the double diode model.

Table 1 also indicates that MPCOA and ABSO rank the overall lowest and second lowest RMSE values among these compared techniques. As the RMSE values of MPCOA and ABSO are very close, we will compare the results of these two techniques in detail. Two indexes, individual absolute error (IAE) and relative error (RE), are used to show the performance with definition as:

$$IAE = |I_{\text{measured}} - I_{\text{estimated}}| = |I_t - I'_t| \quad (16)$$

$$RE = \frac{I_{\text{measured}} - I_{\text{estimated}}}{I_{\text{measured}}} = \frac{I_t - I'_t}{I_t} \quad (17)$$

In Table 2, IAE and RE of each measurement using the optimal values  $X^*$  found by MPCOA and ABSO have been summarized.

In Fig. 7, IAE and RE of each measurement using the optimal values  $X^*$  found by MPCOA and ABSO have been illustrated. From both Fig. 7 and Table 2, we can also know that MPCOA has better performance than that of ABSO.

In order to illustrate the quality of the extracted optimal values  $X^*$  found by MPCOA,  $R_s$ ,  $R_{sh}$ ,  $I_{ph}$ ,  $I_{sd1}$ ,  $I_{sd2}$ ,  $n_1$  and  $n_2$  are put into the double diode model in Eq. (2), then the  $I$ – $V$  and  $P$ – $V$  characteristic of this model can be reconstructed. The  $I$ – $V$  and  $P$ – $V$  characteristic resulted from  $X^*$  found by MPCOA along with the real data have been

illustrated in Fig. 8. From the figure, we can see that the reconstructed double diode model is in good agreement with the real data.

## 5.2. Case study 2: single diode model

This case demonstrates the ability of MPCOA to extract parameters of the single diode model. The 26 pairs real  $V$ – $I$  values and other conditions are the same as in case 1. The convergence process of the MPCOA during the parameter extraction process for the single diode model is plotted in

Table 2

IAE and RE using extracted optimal values  $X^*$  found by MPCOA and ABSO (double diode model).

Meas.	$V_t$ (V)	$I_t$ (A)	ABSO			MPCOA		
			$I'_t$ (A)	IAE	RE	$I'_t$ (A)	IAE	RE
1	−0.2057	0.764	0.764031	0.00031	−4.02e−05	0.764055	0.000055	−0.00007
2	−0.1291	0.762	0.762629	0.000629	−0.00083	0.762644	0.000644	−0.00084
3	−0.0588	0.7605	0.761343	0.000843	−0.00111	0.761349	0.000849	−0.00111
4	0.0057	0.7605	0.760162	0.000338	0.000445	0.760160	0.000340	0.00044
5	0.0646	0.76	0.75908	0.00092	0.00121	0.759072	0.000928	0.00122
6	0.1185	0.759	0.758081	0.000919	0.00121	0.758069	0.000931	0.00122
7	0.1678	0.757	0.757139	0.000139	−0.00018	0.757126	0.000126	−0.00016
8	0.2132	0.757	0.756193	0.000807	0.001066	0.756182	0.000818	0.00107
9	0.2545	0.7555	0.755132	0.000368	0.000487	0.755131	0.000369	0.00048
10	0.2924	0.754	0.753694	0.000306	0.000406	0.753708	0.000292	0.00038
11	0.3269	0.7505	0.751392	0.000892	−0.00119	0.751375	0.000875	−0.00116
12	0.3585	0.7465	0.747322	0.000822	−0.0011	0.747373	0.000873	−0.00117
13	0.3873	0.7385	0.740044	0.001544	−0.00209	0.740104	0.001604	−0.00216
14	0.4137	0.728	0.727331	0.000669	0.000919	0.727383	0.000617	0.00084
15	0.4373	0.7065	0.706896	0.000396	−0.00056	0.706920	0.000420	−0.00059
16	0.459	0.6755	0.675265	0.000235	0.000348	0.675248	0.000252	0.00037
17	0.4784	0.632	0.630889	0.001111	0.001758	0.630833	0.001167	0.00184
18	0.496	0.573	0.572114	0.000886	0.001546	0.572038	0.000962	0.00167
19	0.5119	0.499	0.499533	0.000533	−0.00107	0.499461	0.000461	−0.00092
20	0.5265	0.413	0.413525	0.000525	−0.00127	0.413482	0.000482	−0.00116
21	0.5398	0.3165	0.31723	0.00073	−0.00231	0.317224	0.000724	−0.00228
22	0.5521	0.212	0.21209	0.00009	−0.00042	0.212119	0.000119	−0.00056
23	0.5633	0.1035	0.102694	0.000806	0.007788	0.102741	0.000759	0.00733
24	0.5736	−0.01	−0.00927	0.00073	0.07253	−0.009345	0.00655	0.06552
25	0.5833	−0.123	−0.12439	0.00139	−0.01126	−0.124383	0.001383	−0.01124
26	0.59	−0.21	−0.20917	0.00083	0.003965	−0.209207	0.000793	0.00377

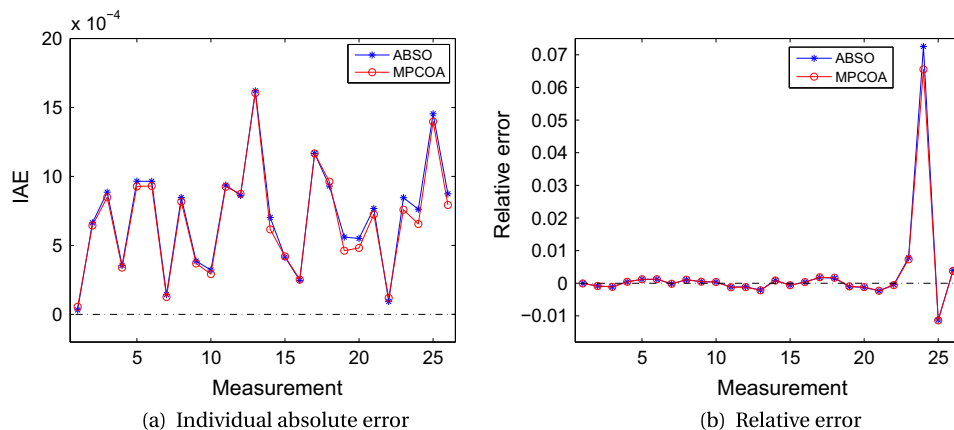


Fig. 7. IAE and RE using extracted optimal values  $X^*$  found by MPCOA and ABSO (double diode model).



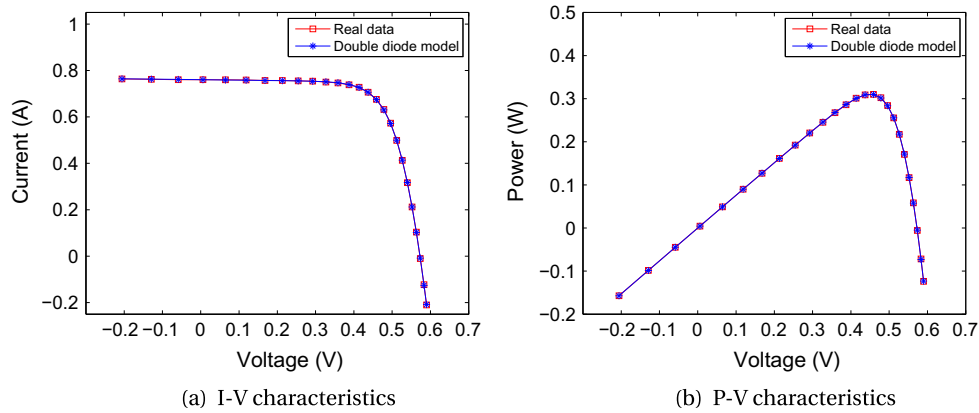


Fig. 8. Comparison results from the real data and the double diode model.

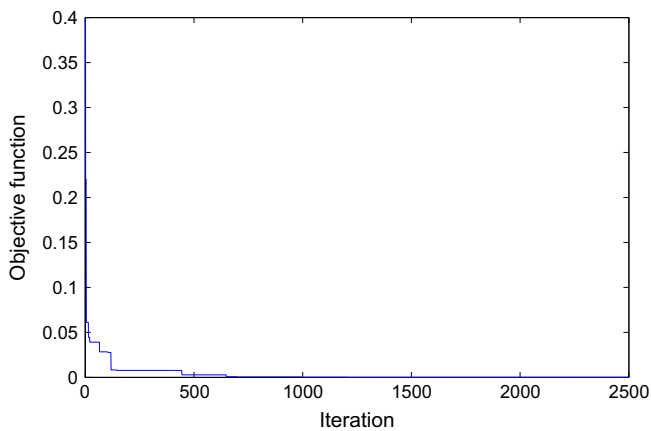


Fig. 9. Convergence process of MPCOA during the parameter extraction process of the single diode model.

Fig. 9, indicating the global optimal value of the objective function as in Eq. (8) during the iterations.

Extracted optimal parameters values  $X^*$  and RMSE value for the single diode model of MPCOA have been shown in Table 3. Here MPCOA is compared with several other techniques, they are: artificial bee swarm optimization (ABSO) (Askarzadeh and Rezazadeh, 2013), chaos particle swarm optimization (CPSO) (Huang et al., 2011), genetic algorithm (GA) (AlRashidi et al., 2011), pattern search (PS) (AlHajri et al., 2012), simulated annealing (SA) (El-Naggar et al., 2012), and harmony search algorithm (HSA) (Askarzadeh and Rezazadeh, 2013).

The extracted optimal parameters values  $X^*$  and RMSE value for the single diode model using these techniques have been summarized in Table 3. From Table 3, we can see that the MPCOA provides the lowest RMSE value ( $9.4457\text{e}-4$ ) among these techniques, followed by ABSO, HSA, CPSO, PS, SA, and GA. Since MPCOA has found the minimum RMSE value, we can conclude that MPCOA outperforms ABSO, CPSO, GA, PS, SA, and HSA. As a result, the optimal values  $X^*$  found by MPCOA are closer to the real ones for the single diode model.

Table 3 also indicates that MPCOA and ABSO rank the overall lowest and second lowest RMSE values among these compared techniques. As the RMSE values of MPCOA and ABSO are very close, we will compare the results of these two techniques in detail. Two indexes, IAE and RE, are also used to show the performance. In Table 4, IAE and RE of each measurement using the optimal values  $X^*$  found by MPCOA and ABSO have been summarized.

In Table 4, IAE and RE of each measurement using the optimal values  $X^*$  found by MPCOA and ABSO have been calculated. Fig. 10 illustrates the IAE and RE of each measurement using the optimal values  $X^*$  found by MPCOA and ABSO. From both Fig. 10 and Table 4, we can also know that MPCOA has better performance than that of ABSO.

In order to illustrate the quality of the extracted optimal values  $X^*$  found by MPCOA,  $R_s$ ,  $R_{sh}$ ,  $I_{ph}$ ,  $I_{sd}$  and  $n$  are put into the single diode model in Eq. (3), then the  $I-V$  and  $P-V$  characteristic of the single diode model can be recon-

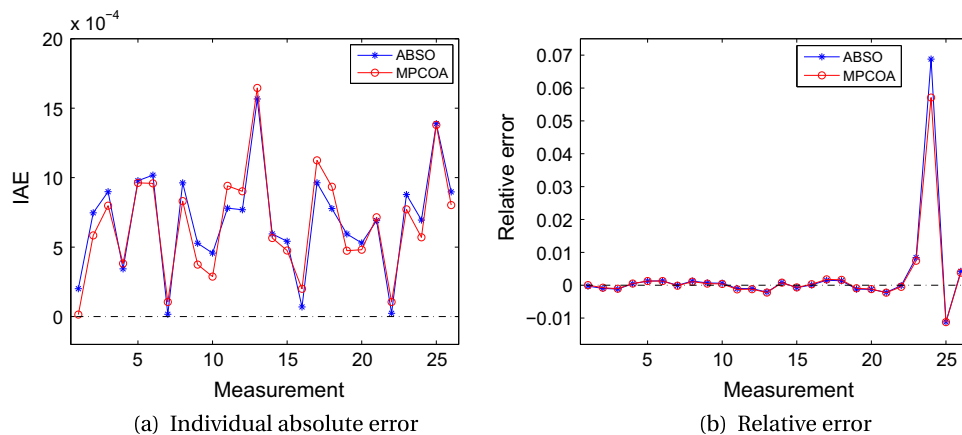
Table 3  
Comparison among different parameter extraction techniques for the single diode model.

Item	MPCOA	ABSO	CPSO	GA	P	SA	HSA
$R_s$ ( $\Omega$ )	0.03635	0.03659	0.0354	0.0299	0.0313	0.0345	0.03663
$R_{sh}$ ( $\Omega$ )	54.6328	52.2903	59.012	42.3729	64.1026	43.1034	53.5946
$I_{ph}$ (A)	0.76073	0.76080	0.7607	0.7619	0.7617	0.7620	0.76070
$I_{sd}$ ( $\mu\text{A}$ )	0.32655	0.30623	0.4000	0.8087	0.9980	0.4798	0.30495
$n$	1.48168	1.47583	1.5033	1.5751	1.6000	1.5172	1.47538
RMSE	$9.4457\text{e}-4$	$9.9124\text{e}-4$	0.00139	0.01908	0.01494	0.01900	$9.9510\text{e}-4$

Table 4

IAE and RE using extracted optimal values  $X^*$  found by MPCOA and ABSO (single diode model).

Meas.	$V_t$ (V)	$I_t$ (A)	ABSO algorithm			MPCOA algorithm		
			$I'_t$ (A)	IAE	RE	$I'_t$ (A)	IAE	RE
1	−0.2057	0.764	0.764201	0.000201	−0.00026	0.763985	0.000015	0.00002
2	−0.1291	0.762	0.762737	0.000737	−0.00097	0.762584	0.000584	−0.00076
3	−0.0588	0.7605	0.761393	0.000893	−0.00117	0.761298	0.000798	−0.00105
4	0.0057	0.7605	0.76016	0.00034	0.000447	0.760117	0.000383	0.00050
5	0.0646	0.76	0.759032	0.000968	0.001274	0.759037	0.000963	0.00126
6	0.1185	0.759	0.757992	0.001008	0.001328	0.758041	0.000959	0.00126
7	0.1678	0.757	0.757017	0.000017	−2.21e−05	0.757105	0.000105	−0.00014
8	0.2132	0.757	0.756047	0.000953	0.001259	0.756169	0.000831	0.00109
9	0.2545	0.7555	0.754977	0.000523	0.000692	0.755125	0.000375	0.00049
10	0.2924	0.754	0.753547	0.000453	0.0006	0.753712	0.000288	0.00038
11	0.3269	0.7505	0.751277	0.000777	−0.00103	0.751441	0.000941	−0.00125
12	0.3585	0.7465	0.74726	0.00076	−0.00102	0.747402	0.000902	−0.00121
13	0.3873	0.7385	0.740051	0.001551	−0.0021	0.740145	0.001645	−0.00222
14	0.4137	0.728	0.727411	0.000589	0.000809	0.727434	0.000566	0.00077
15	0.4373	0.7065	0.707033	0.000533	−0.00076	0.706975	0.000475	−0.00067
16	0.459	0.6755	0.675431	0.000069	0.000102	0.675300	0.000200	0.00030
17	0.4784	0.632	0.631046	0.000954	0.001509	0.630875	0.001125	0.00178
18	0.496	0.573	0.57223	0.00077	0.001344	0.572065	0.000935	0.00163
19	0.5119	0.499	0.499591	0.000591	−0.00118	0.499474	0.000474	−0.00095
20	0.5265	0.413	0.413524	0.000524	−0.00127	0.413481	0.000481	−0.00116
21	0.5398	0.3165	0.317184	0.000684	−0.00216	0.317214	0.000714	−0.00226
22	0.5521	0.212	0.212023	0.000023	−0.00011	0.212105	0.000105	−0.00049
23	0.5633	0.1035	0.10263	0.00087	0.008404	0.102728	0.000772	0.00745
24	0.5736	−0.01	−0.00931	0.00069	0.068809	−0.009429	0.000571	0.05708
25	0.5833	−0.123	−0.12438	0.00138	−0.01118	−0.124378	0.001378	−0.01121
26	0.59	−0.21	−0.20911	0.00089	0.00423	−0.209197	0.000803	0.00382

Fig. 10. IAE and RE using extracted optimal values  $X^*$  found by MPCOA and ABSO (single diode model).

structed. The  $I$ – $V$  and  $P$ – $V$  characteristic resulted from extracted optimal values  $X^*$  by MPCOA along with the real data have been illustrated in Fig. 11. From the figure, we can see that the reconstructed double diode model is in good agreement with the real data.

### 5.3. Case study 3: PV module

In this case, real  $V$ – $I$  values of PV module as the same as in AlRashidi et al. (2011) are used as the measurements, which are derived from a 36 polycrystalline silicon cells which are connected in series under 1 sun ( $1000 \text{ W/m}^2$ ) at

45 °C. In this simulation, these measurements are used to extract the PV model parameters by the MPCOA.

Extracted optimal parameters values  $X^*$  and RMSE value for the PV module by the MPCOA have been reported in Table 5. Here MPCOA is also compared with several other techniques, they are: Newton (Easwarakhanthan et al., 1986), method in Bouzidi et al. (2007), CPSO (Huang et al., 2011), method in Chegaar et al. (2008), PS (AlRashidi et al., 2011), and SA (El-Naggar et al., 2012).

The comparison among different parameter extraction techniques for the PV module has been summarized in Table 5. It can be seen from Table 5 that like the previous

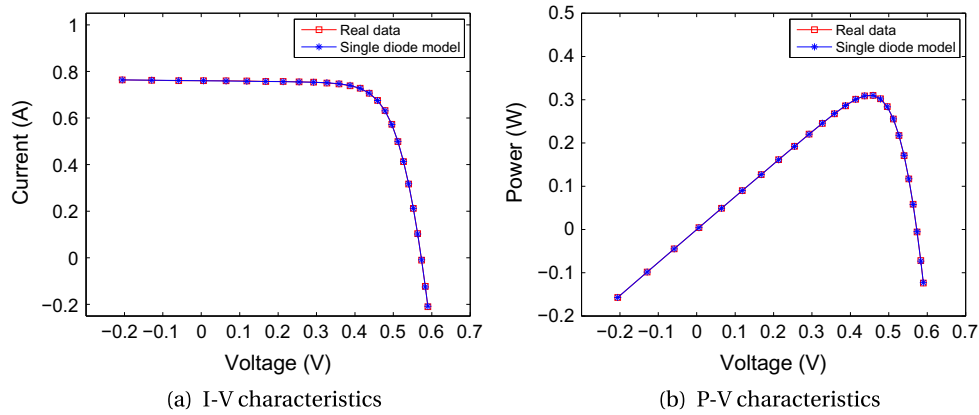


Fig. 11. Comparison results from the real data and the single diode model.

Table 5

Comparison among different parameter extraction techniques for the PV module.

Item	MPCOA	Newton	Bouzi et al. (2007)	CPSO	Chegaar et al. (2008)	PS	SA
$I_{ph}$ (A)	1.03188	1.0318	1.0339	1.0286	1.0310	1.0313	1.0331
$I_{sd}$ ( $\mu$ A)	3.37370	3.2875	3.0760	8.3010	3.8236	3.1756	3.6642
$R_s$ ( $\Omega$ )	1.20295	1.2057	1.2030	1.0755	1.0920	1.2053	1.1989
$R_{sh}$ ( $\Omega$ )	849.6927	555.5556	555.5556	1850.1000	689.6600	714.2857	833.3333
$n$	48.50646	48.4500	48.1862	52.2430	48.9300	48.2889	48.8211
RMSE	0.002425	0.7805	0.6130	0.0035	0.0102	0.0118	0.0027

Table 6

IAEs based on the extracted parameters (PV module).

Item	$V_t$ (V)	$I_t$ (A)	MPCOA	Newton	PS	Bouzi et al. (2007)	SA
1	0.1248	1.0315	0.00123	0.00213	0.00220	0.00008	0.00006
2	1.8093	1.0300	0.00173	0.00303	0.00378	0.00165	0.00064
3	3.3511	1.0260	0.00038	0.00127	0.00265	0.00050	0.00141
4	4.7622	1.0220	0.00252	0.00056	0.00141	0.00077	0.00349
5	6.0538	1.0180	0.00451	0.00226	0.00024	0.00197	0.00541
6	7.2364	1.0155	0.00447	0.00199	0.00101	0.00124	0.00529
7	8.3189	1.0140	0.00226	0.00042	0.00388	0.00155	0.00296
8	9.3097	1.0100	0.00029	0.00253	0.00642	0.00399	0.00083
9	10.2163	1.0035	0.00308	0.00602	0.01032	0.00772	0.00282
10	11.0449	0.9880	0.00364	0.00660	0.01126	0.00844	0.00370
11	11.8018	0.9630	0.00357	0.00650	0.01145	0.00837	0.00403
12	12.4929	0.9255	0.00267	0.00544	0.01059	0.00722	0.00350
13	13.1231	0.8725	0.00007	0.00235	0.00756	0.00393	0.00100
14	13.6983	0.8075	0.00028	0.00231	0.00742	0.00360	0.00152
15	14.2221	0.7265	0.00141	0.00012	0.00471	0.00082	0.00044
16	14.6995	0.6345	0.00196	0.00125	0.00309	0.00068	0.00122
17	15.1346	0.5345	0.00121	0.00062	0.00307	0.00040	0.00036
18	15.5311	0.4275	0.00133	0.00115	0.00173	0.00126	0.00080
19	15.8929	0.3185	0.00018	0.00039	0.00234	0.00001	0.00074
20	16.2229	0.2085	0.00063	0.00161	0.00255	0.00103	0.00189
21	16.5241	0.1010	0.0010	0.00521	0.00505	0.00448	0.00534
22	16.7987	-0.0080	0.00016	0.00056	0.00067	0.00023	0.00059
23	17.0499	-0.1110	0.00003	0.00005	0.00228	0.00075	0.00006
24	17.2793	-0.2090	0.00012	0.00024	0.00319	0.00052	0.00000
25	17.4885	-0.3030	0.00098	0.00227	0.00675	0.00296	0.00262
Total IAE			0.03977	0.05688	0.11561	0.06418	0.05071

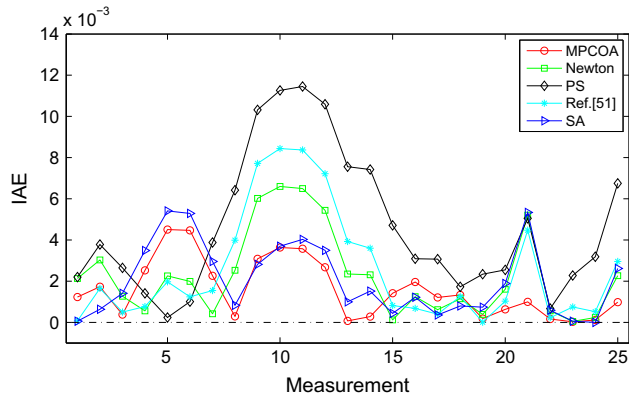


Fig. 12. IAE using extracted optimal values  $X^*$  found by different techniques (PV module).

cases, MPCOA also gets the lowest RMSE value (**0.002425**) among these techniques, followed by SA, CPSO, method in Chegaar et al. (2008), PS, method in Bouzidi et al. (2007), and Newton. Since MPCOA has found the minimum RMSE value in the parameter extraction of the PV module, we can conclude that MPCOA outperforms SA, CPSO, method in Chegaar et al. (2008), PS, method in Bouzidi et al. (2007), and Newton.

Table 6 and Fig. 12 have also summarized the IAE of each measurement using the extracted optimal parameters values  $X^*$  found by MPCOA, Newton, PS, method in Bouzidi et al. (2007), and SA. The total-IAE, which is the summarize of IAE for each measurement is also

computed in Table 6. The results in Table 6 also indicate that the extracted optimal parameters values  $X^*$  found by MPCOA gets the lowest total-IAE value (**0.03977**) among these techniques for the PV module. The simulation results in Table 6 and Fig. 12 indicate that MPCOA outperforms Newton, PS, method in Bouzidi et al. (2007), and SA for this parameter extraction problem.

In order to illustrate the quality of the extracted optimal values  $X^*$  found by MPCOA,  $X^*$  is used to reconstruct  $I$ – $V$  characteristic of the PV module, and the reconstructed  $I$ – $V$  characteristic is illustrated in Fig. 13. According the  $I$ – $V$  characteristic shown in Fig. 13, we can know that the reconstructed  $I$ – $V$  characteristic using extracted optimal values found by MPCOA fit the real data very well.

#### 5.4. Experiment test

Here the proposed MPCOA technique for the parameter extraction of solar cell models has been tested with experiments. The experimental data from multi-crystalline KC 200GT type Solar Panel are used to test the model of double diode model and single diode model, and the experimental data from mono-crystalline SQ 150-PC type are used to test the model of PV module. The experimental data are collected at five different irradiance levels, namely  $1000 \text{ W/m}^2$ ,  $800 \text{ W/m}^2$ ,  $400 \text{ W/m}^2$ ,  $400 \text{ W/m}^2$ , and  $200 \text{ W/m}^2$ . The variations in temperature are not considered for brevity. The MPCOA parameters have the same values with the former simulation. Experiment results using the proposed parameter extraction technique for different solar cell models at  $1000 \text{ W/m}^2$  are shown in Table 7. The extracted parameters of solar cell models using the experimental data are also reported. It can be seen from Table 7 that the RMSE is very small for different solar cell models.

The blue star line in Fig. 14 shows the current–voltage ( $I$ – $V$ ) curves generated using the parameters obtained by the MPCOA. It can be seen that the extraction results in  $I$ – $V$  curves that accurately fit the whole range of experimental data. In particular, the accuracies at low irradiance level also match well. Accurate extraction of solar cell models parameters at low irradiance is very crucial when the module is subjected certain mismatch conditions, for example partial shading.

From the experiment results for different solar cell models in Table 7 and Fig. 14, the parameter extraction performance of the proposed MPCOA technique is verified with good accuracy. This also shows the good performance of the proposed MPCOA technique.

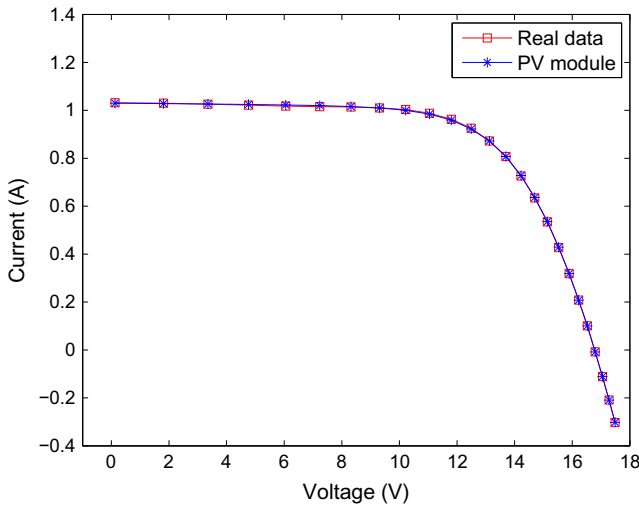


Fig. 13. Comparison results from the real data and the PV module.

Table 7  
Experiment results using the proposed parameter extraction technique.

Model	Type	Current (A)	Resistance ( $\Omega$ )	Ideality factor	RMSE
Double diode model	KC 200GT	$I_{ph} = 8.21$ , $I_{sd1} = 4.25e - 10$ , $I_{sd2} = 4.28e - 10$	$R_s = 0.32$ , $R_{sh} = 160.6$	$n_1 = 1.01$ , $n_2 = 1.29$	0.021
Single diode model	KC 200GT	$I_{ph} = 8.21$ , $I_{sd} = 4.28e - 10$	$R_s = 0.32$ , $R_{sh} = 161.1$	$n = 1.02$	0.023
PV module	SQ 150-PC	$I_{ph} = 4.80$ , $I_{sd} = 3.22e - 10$	$R_s = 0.91$ , $R_{sh} = 276.2$	$n = 1.01$	0.026

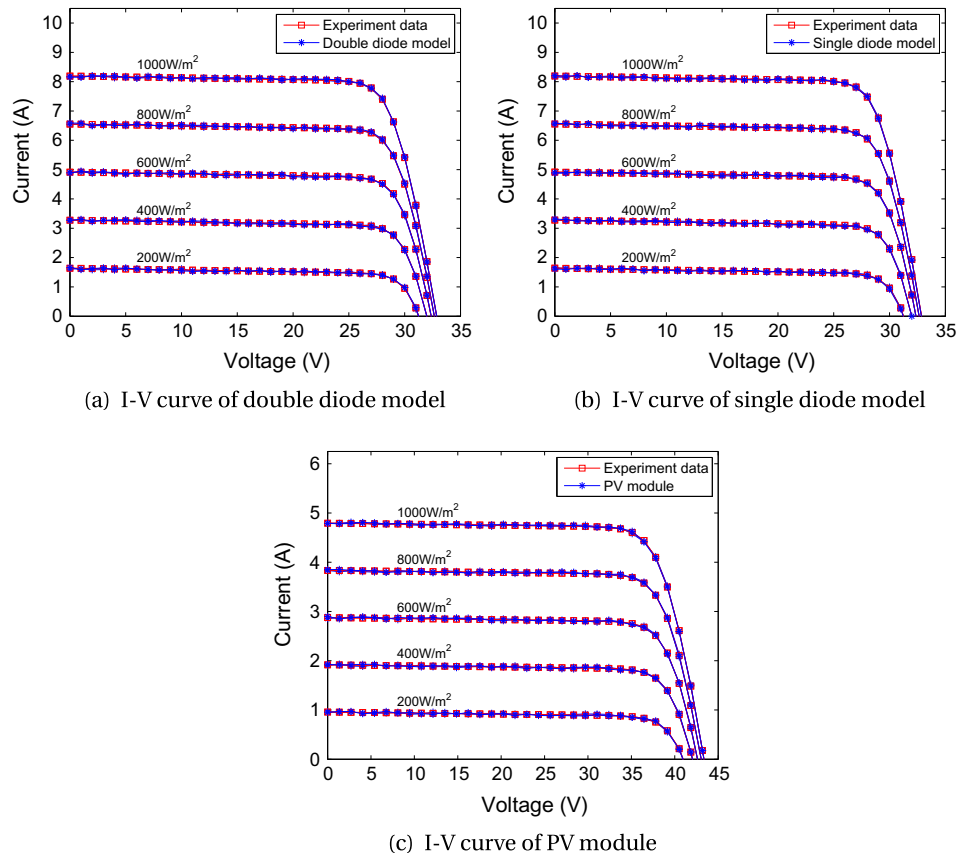


Fig. 14.  $I$ – $V$  curve of the experimental data and the extracted solar cell models.

## 6. Conclusion

This article proposes a novel MPCOA technique for the parameter extraction of solar cell models. The proposed MPCOA technique provides a good balance between exploration and exploitation. In the simulation and experiment, MPCOA technique is applied to extract the parameters of different solar cell models, i.e., double diode, single diode, and PV module. Comparison results are in favor of MPCOA, which outperforms other meta-heuristic algorithms, such as GA, CPSO, ABSO, SA, PS, HSA. The proposed new technique provides another optional method to extract parameters of solar cell models.

## References

- AbdulHadi, M., Al-Ibrahim, A.A., Virk, G.S., 2004. Neuro-fuzzy-based solar cell model. *IEEE Trans. Energy Convers.* 19 (3), 619–624.
- AlHajri, M.F., El-Naggar, K.M., AlRashidi, M.R., Al-Othman, A.K., 2012. Optimal extraction of solar cell parameters using pattern search. *Renew. Energy* 44, 238–245.
- AlRashidi, M.R., AlHajri, M.F., El-Naggar, K.M., Al-Othman, A.K., 2011. A new estimation approach for determining the  $I$ – $V$  characteristics of solar cells. *Solar Energy* 85 (7), 1543–1550.
- Amrouche, B., Guessoum, A., Belhamel, M., 2012. A simple behavioural model for solar module electric characteristics based on the first order system step response for MPPT study and comparison. *Appl. Energy* 91 (1), 395–404.
- Askarzadeh, A., Rezazadeh, A., 2013. Artificial bee swarm optimization algorithm for parameters identification of solar cell models. *Appl. Energy* 102 (SI), 943–949.
- Bayhan, H., Bayhan, M., 2011. A simple approach to determine the solar cell diode ideality factor under illumination. *Solar Energy* 85 (5), 769–775.
- Bonanno, F., Capizzi, G., Graditi, G., Napoli, C., Tina, G.M., 2012. A radial basis function neural network based approach for the electrical characteristics estimation of a photovoltaic module. *Appl. Energy* 97 (SI), 956–961.
- Bouzidi, K., Chegaar, M., Nehaoua, N., 2007. New method to extract the parameters of solar cells from their illuminated  $I$ – $V$  curve. In: 4th International Conference on Computer Integrated Manufacturing, Setif, Algeria.
- Chan, D.S.H., Phillips, J.R., Phang, J.C.H., 1986. A comparative-study of extraction methods for solar-cell model parameters. *Solid-State Electron.* 29 (3), 329–337.
- Chegaar, M., Nehaoua, N., Bouhemadou, A., 2008. Organic and inorganic solar cells parameters evaluation from single  $I$ – $V$  plot. *Energy Convers. Manage.* 49 (6), 1376–1379.
- Chen, Y.F., Wang, X.M., Li, D., Hong, R.J., Shen, H., 2011. Parameters extraction from commercial solar cells  $I$ – $V$  characteristics and shunt analysis. *Appl. Energy* 88 (6), 2239–2244.
- Cubas, J., Pindado, S., Victoria, M., 2014. On the analytical approach for modeling photovoltaic systems behavior. *J. Power Sources* 247, 467–474.
- Das, A.K., 2012. Analytical derivation of explicit  $J$ – $V$  model of a solar cell from physics based implicit model. *Solar Energy* 86 (1), 26–30.
- Easwarakhanthan, T., Bottin, J., Bouhouch, I., Boutrif, C., 1986. Nonlinear minimization algorithm for determining the solar cell parameters with microcomputers. *Solar Energy* 4 (1), 1–12.



- El-Naggar, K.M., AlRashidi, M.R., AlHajri, M.F., Al-Othman, A.K., 2012. Simulated annealing algorithm for photovoltaic parameters identification. *Solar Energy* 86 (1), 266–274.
- Fathabadi, H., 2013. Novel neural-analytical method for determining silicon/plastic solar cells and modules characteristics. *Energy Convers. Manage.* 76, 253–259.
- Ghani, F., Duke, M., Carson, J., 2013. Numerical calculation of series and shunt resistance of a photovoltaic cell using the Lambert W-function: experimental evaluation. *Solar Energy* 87, 246–253.
- Ghani, F., Duke, M., Carson, J., 2013. Numerical calculation of series and shunt resistances and diode quality factor of a photovoltaic cell using the Lambert W-function. *Solar Energy* 91, 422–431.
- Gong, W., Cai, Z., 2013. Parameter extraction of solar cell models using repaired adaptive differential evolution. *Solar Energy* 94, 209–220.
- Hachana, O., Hemsas, K.E., Tina, G.M., Ventura, C., 2013. Comparison of different metaheuristic algorithms for parameter identification of photovoltaic cell/module. *J. Renew. Sust. Energy* 5 (5), 053122.
- Huang, W., Jiang, C., Xue, L., Song, D., 2011. Extracting solar cell model parameters based on chaos particle swarm algorithm. In: *Proceedings of International Conference on Electric Information and Control Engineering (ICEICE)*, pp. 398–402.
- Ishaque, K., Salam, Z., Mekhilef, S., Shamsudin, A., 2012. Parameter extraction of solar photovoltaic modules using penalty-based differential evolution. *Appl. Energy* 99, 297–308.
- Jain, A., Kapoor, A., 2004. Exact analytical solutions of the parameters of real solar cells using Lambert W-function. *Sol. Energy Mater. Sol. Cells* 81 (2), 69–277.
- Jain, A., Kapoor, A., 2005. A new approach to study organic solar cell using Lambert W-function. *Sol. Energy Mater. Sol. Cells* 86 (2), 197–205.
- Jain, A., Sharma, S., Kapoor, A., 2006. Solar cell array parameters using Lambert W-function. *Sol. Energy Mater. Sol. Cells* 90 (1), 25–31.
- Jervase, J.A., Bourdouce, H., Al-Lawati, A., 2001. Solar cell parameter extraction using genetic algorithms. *Measure. Sci. Technol.* 12 (11), 1922–1925.
- Karatepe, E., Boztepe, M., Colak, M., 2006. Neural network based solar cell model. *Energy Convers. Manage.* 47 (9–10), 1159–1178.
- Karmalkar, S., Haneefa, S., 2008. A physically based explicit  $J-V$  model of a solar cell for simple design calculations. *IEEE Electron Device Lett.* 29 (5), 449–451.
- Khan, F., Baek, S.H., Park, Y., Kim, J.H., 2013. Extraction of diode parameters of silicon solar cells under high illumination conditions. *Energy Convers. Manage.* 76, 421–429.
- Kim, W., Choi, W., 2010. A novel parameter extraction method for the one-diode solar cell model. *Solar Energy* 84 (6), 1008–1019.
- Li, B., Jiang, W., 1998. Optimizing complex function by chaos search. *Cybernet. Syst.* 29 (4), 409–419.
- Lun, S.X., Du, C.J., Yang, G.H., Wang, S., Guo, T.T., Sang, J.S., Li, J.P., 2013. An explicit approximate  $I-V$  characteristic model of a solar cell based on padé approximants. *Solar Energy* 92, 147–159.
- Lun, S.X., Du, C.J., Guo, T.T., Wang, S., Sang, J.S., Li, J.P., 2013. A new explicit  $I-V$  model of a solar cell based on Taylor's series expansion. *Solar Energy* 94, 221–232.
- Okamoto, T., Hirata, H., 2013. Global optimization using a multipoint type quasi-chaotic optimization method. *Appl. Soft Comput.* 13 (2), 1247–1264.
- Orioli, A., Gangi, A.D., 2013. A procedure to calculate the five-parameter model of crystalline silicon photovoltaic modules on the basis of the tabular performance data. *Appl. Energy* 102 (SI), 1160–1177.
- Ortiz-Conde, A., Sanchez, F.J.G., 2005. Extraction of non-ideal junction model parameters from the explicit analytic solutions of its  $I-V$  characteristics. *Solid-State Electron.* 49 (3), 465–472.
- Ortiz-Conde, A., Sanchez, F.J.G., Muci, J., 2006. New method to extract the model parameters of solar cells from the explicit analytic solutions of their illuminated  $I-V$  characteristics. *Sol. Energy Mater. Sol. Cells* 90 (3), 352–361.
- Patra, J.C., 2011. Neural network-based model for dual-junction solar cells. *Prog. Photovoltaics* 19 (1), 33–44.
- Patra, J.C., 2011a. Chebyshev neural network-based model for dual-junction solar cells. *IEEE Trans. Energy Convers.* 26 (1), 132–139.
- Peng, L.L., Sun, Y.Z., Meng, Z., Wang, Y.L., Xu, Y., 2013. A new method for determining the characteristics of solar cells. *J. Power Sources* 227, 131–136.
- Saleem, H., Karmalkar, S., 2009. An analytical method to extract the physical parameters of a solar cell from four points on the illuminated  $J-V$  curve. *IEEE Electron Device Lett.* 30 (4), 349–352.
- Sandrolini, L., Artioli, M., Reggiani, U., 2010. Numerical method for the extraction of photovoltaic module double-diode model parameters through cluster analysis. *Appl. Energy* 87 (2), 442–451.
- Syafaruddin, Karatepe, E., Hiyama, T., 2012. Fuzzy wavelet network identification of optimum operating point of non-crystalline silicon solar cells. *Comput. Math. Appl.* 63 (1), 68–82.
- Tian, H.M., Mancilla-David, F., Ellis, K., Muljadi, E., Jenkins, P., 2012. A cell-to-module-to-array detailed model for photovoltaic panels. *Sol. Energy Mater. Solar Cells* 86 (9), 2695–2706.
- Yang, D., Li, G., Cheng, G., 2007. On the efficiency of chaos optimization algorithms for global optimization. *Chaos Soliton. Fract.* 34 (4), 1366–1375.
- Yang, D., Liu, Z., Zhou, J., 2014. Chaos optimization algorithms based on chaotic maps with different probability distribution and search speed for global optimization. *Commun. Nonlinear Sci. Numer. Simul.* 19 (4), 1229–1246.
- Ye, M., Wang, X., Xu, Y., 2009. Parameter extraction of solar cells using particle swarm optimization. *J. Appl. Phys.* 105 (9), 094502.
- Yuan, X., Wang, Y., 2008. Parameter selection of support vector machine for function approximation based on chaos optimization. *J. Syst. Eng. Electron.* 19 (1), 191–197.
- Yuan, X., Yang, Y., Wang, H., 2012. Improved parallel chaos optimization algorithm. *Appl. Math. Comput.* 219 (8), 3590–3599.
- Yuan, X., Zhao, J., Yang, Y., Wang, Y., 2014. Hybrid parallel chaos optimization algorithm with harmony search algorithm. *Appl. Soft Comput.* 17, 12–22.
- Zagrouba, M., Sellami, A., Bouaicha, M., Ksouri, M., 2010. Identification of PV solar cells and modules parameters using the genetic algorithms: application to maximum power extraction. *Solar Energy* 84 (5), 860–866.
- Zhou, W., Yang, H., Fang, Z., 2007. A novel model for photovoltaic array performance prediction. *Appl. Energy* 84 (12), 1187–1198.